

Thermal stability and vibrational spectra of the sheet borate tuzlaite, $\text{NaCa}[\text{B}_5\text{O}_8(\text{OH})_2]\cdot 3\text{H}_2\text{O}$

VLADIMIR BERMANEC,^{1,*} KREŠIMIR FURIĆ,² MAŠA RAJIĆ,³ AND GORAN KNIEWALD⁴

¹Mineraloško petrografske zavod, Geološki odsjek, Prirodoslovno matematički fakultet, Horvatovac bb, HR-10000 Zagreb, Croatia

²Molecular Physics Laboratory, Rudjer Bošković Institute, POB 180, 10002 Zagreb, Croatia

³Brodarski Institut, HR-10000 Zagreb, Croatia

⁴Center for Marine and Environmental Research, Rudjer Bošković Institute, POB 180, 10002 Zagreb, Croatia

ABSTRACT

Tuzlaite, a hydrated pentaborate from the Tuzla evaporite deposit in Bosnia and Herzegovina, was analyzed for water content and loss upon heating using thermal analysis methods and vibrational spectroscopy. The resulting phases were identified by X-ray diffraction. The heating of tuzlaite results in a gradual loss of water over several dehydration steps. Two coordinated H_2O molecules escape at 191 °C. Between 248 and 298 °C two hydroxyl groups are eliminated, with an associated structural transformation. A continuous escape of the third water molecule occurs above 300 °C. A phase relationship model for different hydrated borate minerals implies the possible formation pathway of tuzlaite by sequential polymerization of the borate polyanion.

INTRODUCTION

Tuzlaite, $\text{NaCa}[\text{B}_5\text{O}_8(\text{OH})_2]\cdot 3\text{H}_2\text{O}$, is a type of sheet pentaborate found in the Tušanj salt mine at Tuzla, Bosnia and Herzegovina (Bermanec et al. 1994). The evaporite deposit at Tuzla is the largest rock-salt deposit in the Balkan peninsula. The more or less stratified salt-dome type deposit is of mid-Miocene age, hosted in a sedimentary series of banded halite and anhydrite. Anhydrous and hydrated salts were deposited on tertiary dolomites and marls. The geochemistry of coexisting brines and their saturation states imply that the formation environment may be interpreted in terms of the mixing-zone model, rather than end-member type marine or salt lake deposits (Kniewald et al. 1995). On the other hand, the close relationship of the evaporite series with the associated dolomitic limestones as well as evidence of progressive dolomitization, may reflect their possible formation under evaporative, non-evaporative, or seepage-reflux conditions (Hardie and Eugster 1971).

The major mineral assemblage of the Tuzla rock-salt series consists of halite, thenardite, and anhydrite. The activity of water [$a(\text{H}_2\text{O})$] indicator couple is thenardite-mirabilite. Several accessory minerals, including northupite, are present in varying amounts. The assemblage, as well as possible lithotype indicator minerals, has been studied in detail (Kniewald et al. 1986; Bermanec et al. 1992). Tuzlaite, approved as a new mineral and named to honor the occurrence, was discovered as an accessory mineral of the assemblage (Bermanec et al. 1994). The conditions of its formation and thermodynamic stability are still not fully clear, but there are indications that diagenetic changes could have affected the nucleation kinetics of the normal succession of borate minerals in the sequence, resulting in the precipitation of tuzlaite. Searlesite is the only other boron

containing mineral in the same deposit. The main argument in favor of diagenetic tuzlaite formation is the lack of other precursor borate minerals (i.e., colemanite, kernite, ulexite) and characteristic textures observed in the host sediment (Bermanec et al. 2001). The sequence of borate minerals is highly dependent on the chemical characteristics of the depositional environment. In addition to the primary gypsum (gypsarenite) and syndepositional anhydrite, the formation of borate minerals is largely controlled by the activities of Na, Ca, B, Cl, and water. Different borate minerals often accumulate at the margins and in central areas of evaporite basins (Warren 1999). In this respect, the chemistry of tuzlaite, associated minerals and saline formation waters in the area of the Tuzla evaporite deposit may reflect the water/evaporite interaction during burial.

The aqueous and crystal chemistries of hydrated borate minerals are closely related. Most polyanions that are present in the structures of crystallized hydrated borate minerals also exist in aqueous solution (Ingri 1963; Burns et al. 1995). Primary borate minerals precipitate from solutions saturated with their components, but tuzlaite does not seem to be associated with the primary assemblage. Such a situation is commonly observed in deposits of Neogene age where diagenetic borates appear in mineral assemblages as a result of thermal diagenesis, usually followed by reaction diagenesis (Smith and Medrano 1996). Some transformations of borate minerals, involving a change in the water content of the mineral, are considered to be an effect of reaction diagenesis. They can take place isothermally, and do not require the breaking of O-H or O-B bonds, an initial step in polymerization.

The aim of the present investigation was to clarify the role of water in the crystal structure of tuzlaite and its thermal stability, since water is incorporated in its crystal structure both as interlayer water molecules and as bridging OH groups. A model for the phase relationships of hydrated borate minerals

* E-mail: vberman@public.srce.hr

was set up to define the stability field of tuzlaite, in terms of the chemical activity of water and the activity of the mineral's cationic components.

METHODS AND EXPERIMENTAL CONDITIONS

Thermal measurements were performed using a differential scanning calorimeter (DSC) (TA Instruments, DSC Model 2910) and a simultaneous TGA-DTA analyzer (TA Instruments, SDT Model 2960). The curves were obtained by placing 5 mg samples in open platinum sample cans, with a heating rate of 10 °C/min, under nitrogen gas flowing at a rate of 50 mL/min (for TGA-DTA) and 100 mL/min (for DSC). Both instruments were calibrated at the melting point of indium.

For the excitation of Raman spectra, an argon ion laser (Coherent model Innova 100) was used. The 514.5 nm laser beam was filtered through an Anaspec double-pass premonochromator for the removal of the plasma lines and then focused to a 50 μm spot (1/e value). The total power on the sample was kept at 100 mW. Monocrystals of tuzlaite or clots of the powdered mineral (obtained by sample heating at both 200 and 300 °C) were mounted directly on top of the goniometer head in such a way that only the light scattered from the sample reached the entrance slit of the Raman spectrometer. This was done to avoid weak contributions from glass supports or sample tubes. The scattered light, containing the Raman spectrum, was analyzed under 90° scattering geometry using a computerized triple-monochromator (Dilor model Z24) and was detected with a RCA C31034 photomultiplier. The middle, empty part of the Raman spectrum was not recorded. Data points for the high-frequency portion of the Raman spectrum are at 10 cm⁻¹ intervals and for the low frequency part at 4 cm⁻¹ intervals. For both intervals accumulation time was 4 s per data point, 4 scans were coadded, laser power was 100 mW (514.5 nm line), slits were 500 μm.

Infrared transmission spectra were recorded from 400 to 4000 cm⁻¹ using a Perkin-Elmer FTIR instrument, model 2000, equipped with a tri-glycine-sulfate (TGS) detector. Powdered samples, obtained by fine grinding of intact crystallites or after heating, were pressed into KBr pellets. A blank KBr pellet of approximately the same thickness was used to determine the background spectrum. Twenty scans were run for each spectrum with 1 cm⁻¹ resolution.

X-ray diffraction data sets were collected from 0 to 30° Θ with a Philips X'pert powder diffractometer using CuKα radiation filtered with a graphite monocrystal monochromator. Powder diffraction patterns indexed on the basis of analogy with tuzlaite were used for the calculation of unit cell parameters.

The phase relation diagram for tuzlaite and the other hydrated boron minerals of the system Na-Ca-B-O-H₂O was constructed using the HSC Chemistry for Windows (v.4.0) computer program, using thermodynamic data for borate minerals.

RESULTS AND DISCUSSION

Thermogravimetric measurements

The DSC and TGA curves of tuzlaite, scanned in a range from room temperature up to 500 °C (DSC) and 900 °C (TGA)

are shown in Figure 1. It can be seen that the thermal decomposition of tuzlaite under the applied experimental conditions is a complex, multi-stage process. The DSC curve shows three endothermic and one exothermic peak. We interpret the first endothermic reaction at 191.5 °C as the loss of two water molecules from tuzlaite, since the observed weight loss of 10.40 wt% is very close to the calculated weight fraction of two of the structural water molecules (10.81 wt%). The exothermic peak, with a maximum rate at 280.2 °C, is a result of crystal structure decomposition. This is corroborated by X-ray diffraction data (presented in an upcoming section). Another sample was heated up to 200 °C, cooled down to room temperature, rehydrated with water, and finally analyzed by DSC in the temperature range 25–500 °C to confirm our observations of water loss (Fig. 2). The difference in the two curves is the result of the fact that there are substantially more structural defects in the rehydrated material than in the natural sample, so that the loss of water occurs at a greater rate, probably at sites that are more readily dehydrated during the second heating cycle. However, the starting temperature of the water loss reaction is the same in both cases.

In the temperature range 220–320 °C, two endothermic peaks with maximum rates at 247.8 and 298.7 °C characterize

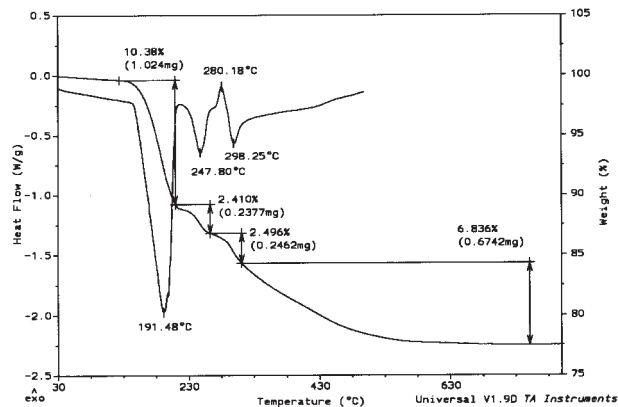


FIGURE 1. DSC and TGA curves of tuzlaite.

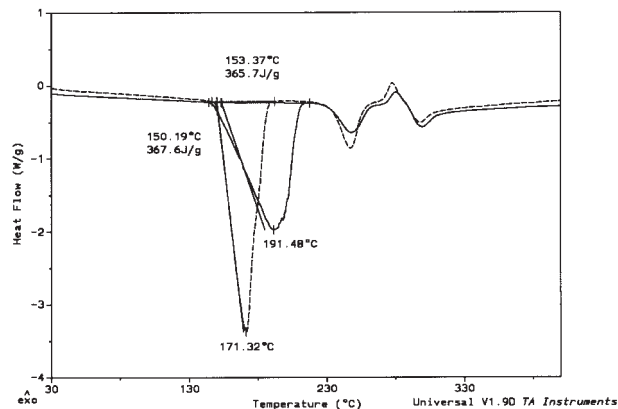


FIGURE 2. Comparison of DSC curves of natural (i.e., unheated) tuzlaite (—) and tuzlaite after heating to 200 °C and subsequent rehydration (---).

the DSC curve. We ascribe the mass loss in these two steps (2.41 and 2.46 wt%) to the stepwise and possibly incomplete liberation of OH anions, situated in two slightly different local environments. The sum of these two weight losses (4.87 wt%) is smaller than weight loss of one OH group (5.72 wt%), implying that a fraction of the first and the second hydroxyl groups remain within the tuzlaite, since there is no explicit evidence that this process is associated with only one of the two formula OH sites, with some of the O atoms probably converting to bridging O atoms. The TGA curve shows an additional mass loss of 6.84 wt% in the temperature range between 300 and 600 °C, which appears somewhat diffuse. This step is related to further dehydroxylation and dehydration of the third water molecule.

A further tuzlaite sample was heated up to 310 °C, then was cooled down to room temperature and the TGA analysis repeated in the range from room temperature to 800 °C (Fig. 3). Above 300 °C the TGA curve of the heated sample quickly starts to follow the TGA curve of an intact (untreated) sample. At approximately 380 °C, the difference Δ between the two curves reaches a constant value nearly equal to the sum of previous water losses. The TGA curve of the previously heated sample exhibits a water loss of 6.4 wt% above 300 °C.

The occurrence of four discrete dehydration steps result in a TGA curve showing three overlapping reactions indicating the complexity of the overall process (Table 1).

Vibrational spectroscopy

A comparison of the complete IR spectrum (400–4000 cm⁻¹) with two Raman spectral intervals (250–1750 and 2850–3850 cm⁻¹), given in Figure 4, shows the complementary nature of the two different techniques. Particularly interesting is the O-H stretching region between 3000 and 3750 cm⁻¹ where IR spectroscopy can be inferior due to strong absorption by molecular water (such a situation is characteristic for aqueous solutions). In the case of tuzlaite, relative intensities and resolved O-H stretching bands are equally present in the Raman and IR spectra. The vibrational spectroscopic results are given in Table 2, including the positions of the observed bands, their assignments, and comments on their relative intensities and shapes. The band

assignments were done following Farmer (1974).

The structure of the stable, well defined form of natural tuzlaite, which exists at atmospheric pressure and within a rather broad temperature interval, is destroyed at elevated temperatures due to the loss of water molecules and hydroxyl groups. These effects of heating were initially observed by TGA measurements, but more details were obtained from vibrational spectroscopic data collected from heated and unheated samples. Raman and infrared spectra of samples heated to 200 and 300 °C were recorded and compared with results obtained for the same sample prior to heating, as shown in Figures 5 and 6.

The vibrational bands in the Raman spectrum of a given sample are generally better resolved (due to narrower peak widths) than in the infrared spectrum of the same sample. However, the infrared spectrum appears to have a higher signal-to-noise ratio and therefore greater sensitivity. The best examples of such behavior can be found in the lower-frequency Raman region up to 900 cm⁻¹ which is characterized by sharp Raman bands and the “fingerprint” region up to 1800 cm⁻¹ characterized by the sensitivity of IR spectroscopy.

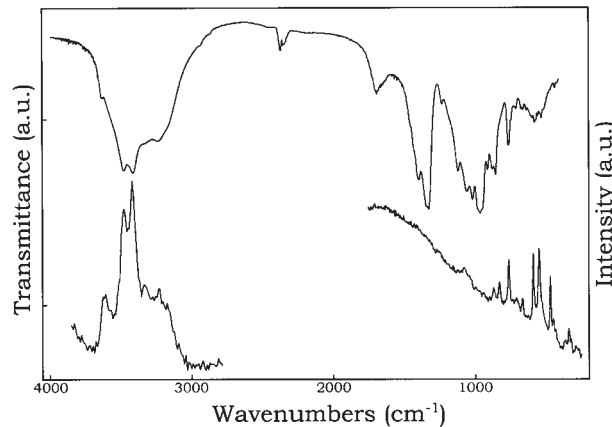


FIGURE 4. Comparison of infrared (upper) and Raman (lower) spectrum of tuzlaite.

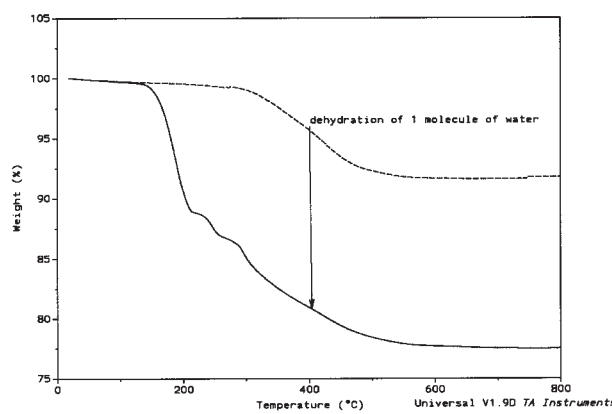


FIGURE 3. TGA curves of natural tuzlaite (—) and tuzlaite after heating to 310°C (— —).

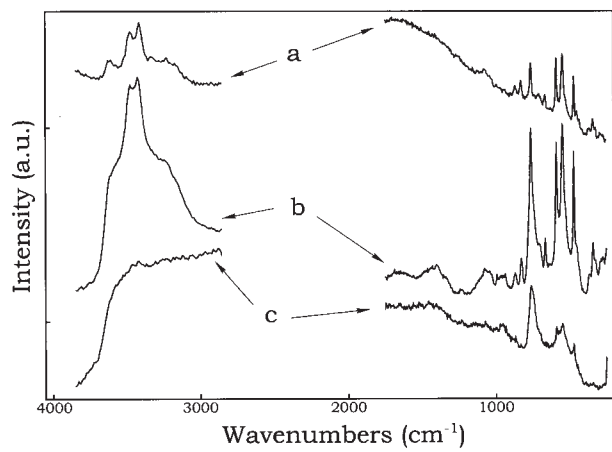


FIGURE 5. Raman spectra of three different samples: (a) natural, (b) after heating to 200 °C, (c) after heating to 300 °C.

TABLE 1. Dehydration and dehydroxylation steps of tuzlaite based on DSC and TGA

DSC thermal effect	T_{\max} °C	Wt loss %	Ea kJ/mol	Process
endothermic	191.48	10.38	91.22	loss of 2 H ₂ O molecules
endothermic	247.80	2.41	214.82	partial elimination of 1 OH group
exothermic	280.18		266.70	structural transformation
endothermic	298.25	2.50	60.41	partial elimination of 1 OH group
no effect (continual loss)	—	6.84	110.41	elimination of 1 H ₂ O molecule and remaining OH

TABLE 2. Positions (in wavenumbers) of Raman and infrared vibrational bands observed for tuzlaite, tuzlaite after heating to 200 °C, and tuzlaite after heating to 300 °C

Raman (cm ⁻¹)	Preliminary assignment			infrared (cm ⁻¹)		
	300 °C	200 °C	original	original	200 °C	300 °C
3620m,sh	3615m		(OH) ₂ stretching	3625m	3628w	
3478vs	3473s			3473vs	3473s	
3425vs	3434s			3410vs	3413s	
3430m,br	3328w		H ₂ O stretching ν_1 and ν_3 , 2 ν_2	3320m	3320m	3370m,br
3225ms	3228w			3225m	3230m	
3150ms	3165w			3160m	3145v	
				1686m	1688w	
				1635w,sh	1690vw	
	1650w,br		H ₂ O bendings (ν_2)	1454w,sh		
					1392vs	
					1338vs	
1385vv,br					1336vs	
					1326vs	
	1398w,br			1322vs	1225w	
	1334w,br				1125w	1380s,vbr
					1112m	
1135vv,br	1232vv	1247vv			1050vs	
	1118vv,sh				1012vs	
1065vv	1075w	1072w			905m,sh	
	1035w,sh	1027w,sh			876m,sh	
	996w,br				853m,sh	
					961vs	
					758m	
					904s	
					707w,sh	
					670w	980s,vbr
					571vw	
					529vw	
	868m	866m				
757m	829m	827m				
701vv	761vs	761m				
586w	707w	704vw				
546w	665m	663				
470w	589vs	589m				
	547vs	546m				
341vv,br	471vs	468m				
		447w				
	366vv	366vw				
	340m	340m				
	325vv	323vw				
	280w	282w	bending modes of trigonal and tetrahedral boron, H ₂ O librations and translations			

TABLE 3. Unit cell parameters for natural tuzlaite, dehydrated and rehydrated materials

Natural tuzlaite	Heated to 191 °C	Rehydrated (after heating)
$a = 6.503(4)$ Å	6.505(8) Å	6.51(1) Å
$b = 13.278(2)$ Å	13.32(2) Å	13.28(1) Å
$c = 11.445(2)$ Å	11.51(2) Å	11.49(2) Å
$\beta = 92.91(2)^\circ$	92.6(1)°	92.5(1)°
$V = 987.0$ Å ³	996(2) Å ³	992(2) Å ³

The infrared background of the natural (i.e., unheated) sample (spectrum a, Fig. 6) is rather flat, but in the Raman spectra an important “hump” appears between 1000 and 2800 cm⁻¹, which screens the expected vibrational bands. Such humps occur frequently in natural samples. Usually they are treated as background fluorescence, probably due to the presence of water (Farmer 1974). The comparison of mentioned spectra with other spectra obtained for heated samples (given in the same figures) shows that bandwidths are lowest for natural samples.

After heating the samples to 200 °C the infrared spectrum is characterized by a broadening of all vibrational bands (spectrum b, Fig. 6) and by intensity loss in the OH stretching region. After such heating, the background of the Raman spectrum is significantly lower allowing the recognition of some bands between 900 and 1750 cm⁻¹ with higher certainty than is the case for the unheated samples (compare the spectra b and a in Fig. 5). Band broadening is a characteristic of the Raman spectrum for the heated sample, as of the IR, particularly for the band due to OH stretching. This effect is somewhat more pronounced for hydroxyl than for H₂O stretching bands. After heating to 300 °C, the broadening of vibrational bands due to all OH entities (hydroxyl groups and coordinated water) result in a single broad band in the 3400 cm⁻¹ region in both Raman and infrared spectra. This band “survives” the heating and affects even the two strongest bands normally appearing around 3450 cm⁻¹. Below 1800 cm⁻¹ very similar effects are observed. The vibrational bands show an additional increase in bandwidth, merging into the very few broad bands centered about 1380, 980, 750, and 550 cm⁻¹. However, on the basis of the vibrational spectra alone, it is impossible to ascertain which OH groups (hydroxyl or molecular water) are the first ones to leave the tuzlaite structure upon heating.

X-ray diffraction

The X-ray powder pattern (Fig. 7) shows that the basic sheet borate structure of tuzlaite is maintained after heating to 200 °C, although the unit cell parameters show a slight increase (Fig. 7 and Table 3), a common effect observed in minerals after dehydration (Armbruster et al. 1989). This implies that the same type of structure is stable with a single water molecule – (i.e., NaCa[B₅O₈(OH)₂]·H₂O). The only important difference is seen on the first diffraction line, the intensity of which decreases with heating, while a new diffraction line appears at a slightly higher Θ value.

Due to the increased background levels in the range be-

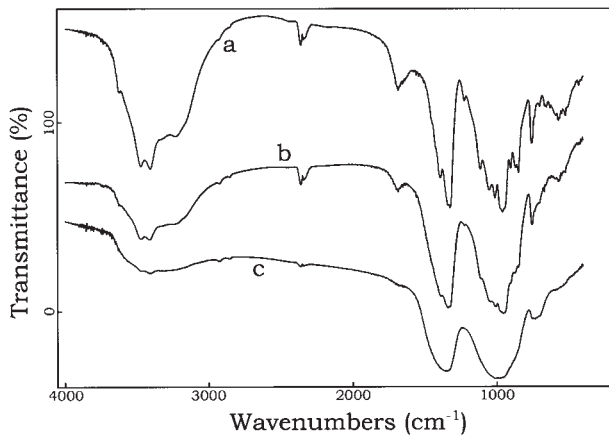


FIGURE 6. Infrared spectra of three different samples: (a) natural, (b) after heating to 200 °C, (c) after heating to 300 °C. The spectra are offset to avoid overlap.

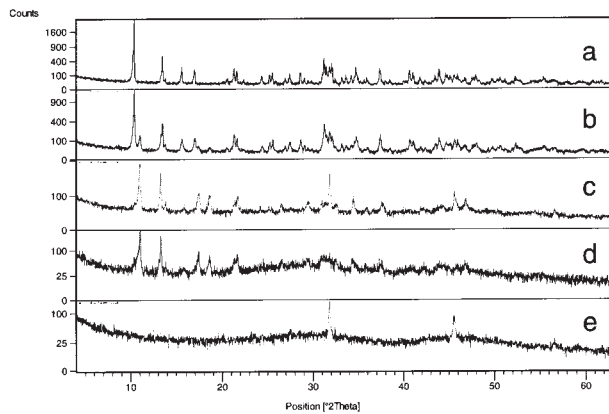


FIGURE 7. X-ray diffraction patterns of (a) tuzlaite, (b) tuzlaite heated to 200 °C, (c) tuzlaite heated to 250 °C, (d) rehydrated tuzlaite, and (e) tuzlaite heated to 300 °C. On (e) all tuzlaite reflections disappear while only halite (always present as an impurity with tuzlaite) maxima remain.

tween 10 and 14° Θ it may also be assumed that some amorphous phases appear after heating of tuzlaite. Partial amorphization is possible due to the dehydration process during the heating steps. However, a subsequent rehydration process decreases the background in this region and the rehydrated phase has sharper diffraction peaks than the dehydrated one. After heating to 300 °C, the sample is amorphous to X-rays.

Phase relationships in the system Na-Ca-B-O-H₂O

A schematic diagram of phase relationships in the system Na-Ca-B-O-H₂O (oxide components) is shown in Figure 8. All solids are in equilibrium with saturated solution. The metastable fields of tincalconite ($\text{Na}_2\text{B}_4\text{O}_7 \cdot 5\text{H}_2\text{O}$) and meyerhoffite ($\text{Ca}_2\text{B}_6\text{O}_{11} \cdot 7\text{H}_2\text{O}$) are delineated with dashed lines. The system is open with respect to water, sodium, and calcium, but closed with respect to boron.

In agreement with mineralogical and petrological evidence from the tuzlaite-bearing host rock (Kniewald et al. 1995), it is

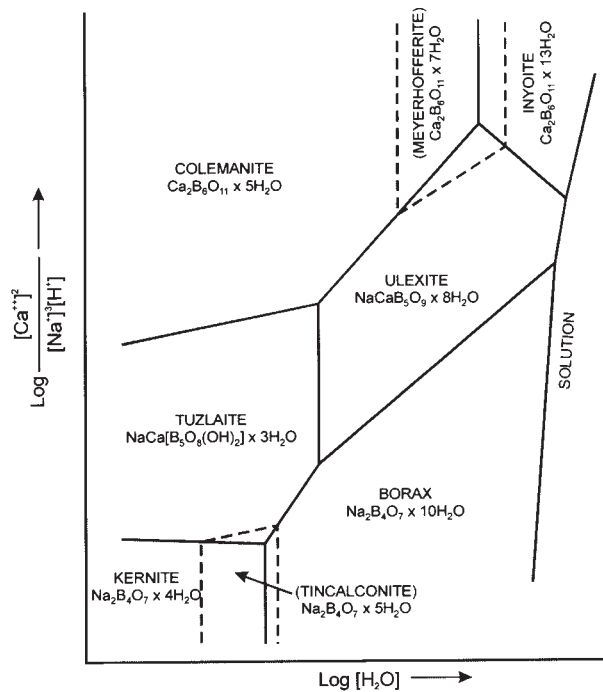
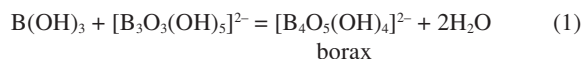
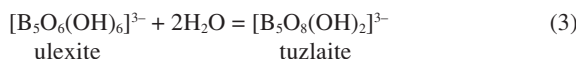
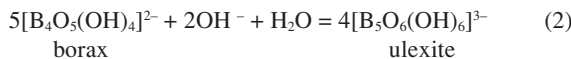


FIGURE 8. Activity-activity diagram for the system $\text{Na}_2\text{O}\cdot 2\text{B}_2\text{O}_3\cdot 4\text{H}_2\text{O} - 2\text{CaO}\cdot 3\text{B}_2\text{O}_3\cdot 5\text{H}_2\text{O} - \text{H}_2\text{O}$.

assumed that this hydrated borate formed initially as a chemical deposit in a saline body of water. Essentially two distinct types of borates form by this mechanism: hydrated sodium borates from alkaline environments high in Na and low in Ca, and hydrated sodium-calcium borates from milieus relatively higher in Ca. These two situations correspond to the conditions for the stability fields of borax and ulexite respectively in activity-activity diagrams, taking into account that the primary borates tend to be the more hydrated phases (Anovitz and Hemingway 1996). The relative abundance of Mg²⁺ in a brine or groundwater at any stage of the paragenetic sequence is a complicating factor, since the actual assemblage formed also depends on Ca²⁺/Mg²⁺ and H₂O concentration. Consequently, a decrease in the activity of water due to concentration of solution by evaporation of water (or due to the influx of a more concentrated solution), or an increase in temperature, would cause dehydration of the primary borate to form a less hydrated phase.

The polymerization of highly hydrated borates requires that the relatively weak O-H bonds be broken. Considering the aqueous chemistry of the borate polyanion, it is quite evident that the pentaborate structure of tuzlaite must have formed from $\text{B}(\text{OH})_3$ by the appropriate number of polymerization steps with the accompanying addition of hydroxyl groups. Thus, the transformation of borax to tuzlaite, via ulexite, may be written in terms of the polyanions





Increasing pH favors the formation of ulexite from borax, while the transformation from ulexite to tuzlaite indicates a diagenetic process, where the formation of the assemblage is largely independent of the alkalinity of the depositional environment.

The data on the thermal instability of tuzlaite in the temperature ranges used in the TGA and DSC measurements imply the importance of both temperature and water activity for tuzlaite formation. Tuzlaite could be a product of such thermal diagenesis followed by reaction diagenesis, but this investigation does not provide sufficient evidence that further polymerization processes resulting in the formation of additional secondary hydrated borate minerals takes place in the formation environment of this mineral.

ACKNOWLEDGMENTS

A part of this study was supported by research grants 119420, 0098132, and 0098303 of the Ministry of Science and Technology of the Republic of Croatia. Comments by G. Rossman, an anonymous reviewer, and the associate editor (C. Merzbacher) helped to improve the manuscript.

REFERENCES CITED

- $5[B_4O_5(OH)_4]^{2-} + 2OH^- + H_2O = 4[B_5O_6(OH)_6]^{3-}$ (2)
borax ulexite

$[B_5O_6(OH)_6]^{3-} + 2H_2O = [B_5O_8(OH)_2]^{3-}$ (3)
ulexite tuzlaite

Increasing pH favors the formation of ulexite from borax, while the transformation from ulexite to tuzlaite indicates a diagenetic process, where the formation of the assemblage is largely independent of the alkalinity of the depositional environment.

The data on the thermal instability of tuzlaite in the temperature ranges used in the TGA and DSC measurements imply the importance of both temperature and water activity for tuzlaite formation. Tuzlaite could be a product of such thermal diagenesis followed by reaction diagenesis, but this investigation does not provide sufficient evidence that further polymerization processes resulting in the formation of additional secondary hydrated borate minerals takes place in the formation environment of this mineral.

ACKNOWLEDGMENTS

A part of this study was supported by research grants 119420, 0098132, and 0098303 of the Ministry of Science and Technology of the Republic of Croatia. Comments by G. Rossman, an anonymous reviewer, and the associate editor (C. Merzbacher) helped to improve the manuscript.

REFERENCES CITED

Anovitz, L.M. and Hemingway, B.S. (1996) Thermodynamics of boron minerals: summary of structural, volumetric and thermochemical data. In L.M.Anovitz and E.S.Grew, Eds., Boron: mineralogy, petrology and geochemistry, 33, 181–261. Reviews in Mineralogy, Mineralogical Society of America, Washington, D.C.

Bermanec, V., Tibljaš, D., Crnjaković, M., and Knewald, G. (1992) Saline minerals of the Tuzla salt deposit as indicators of palaeoceanographic conditions. Rapports de la Commission Internationale pour l'Exploration Scientifique de la Mer Méditerranée, 33, 116. Monaco, Principality of Monaco.

Bermanec, V., Armbruster, T., Tibljaš, D., Sturman, D., and Knewald, G. (1994) Tuzlaite, $NaCa[B_5O_8(OH)_2] \cdot 3H_2O$, a new mineral with a pentaborate sheet structure from the Tuzla salt mine, Bosnia and Herzegovina. American Mineralogist, 79, 562–569.

Bermanec, V., Crnjaković, M., and Knewald, G. (2001) Geochemistry and mineral assemblages of the Mediterranean evaporite deposits 3. Some textural characteristics of evaporite sediments in Tuzla salt deposit. Rapports de la Commission Internationale pour l'Exploration Scientifique de la Mer Méditerranée, 36, 9. Monaco, Principality of Monaco.

Burns, P.C., Grice, J.D., and Hawthorne, F.C. (1995) Borate minerals I. Polyhedral clusters and fundamental building blocks. Canadian Mineralogist, 33, 1131–1151.

Farmer, V.C. (1974) The infrared spectra of minerals. Mineralogical Society Monograph 4, London. 539 p.

Hardie, L.A. and Eugster, H.P. (1971) The depositional environment of marine evaporites: a case for shallow, clastic accumulation. Sedimentology, 16, 187–220.

Ingrin, N. (1963) Equilibrium studies of polyanions containing B^{III} , Si^{IV} , Ge^{IV} , and V^{V} . Svensk Kemisk Tidskrift, 75, 3–34.

Knewald, G., Bermanec, V., and Tibljaš, D. (1986) On the origin and type of the Tuzla salt deposit in Yugoslavia. Rapports de la Commission Internationale pour l'Exploration Scientifique de la Mer Méditerranée, 30/2, 72. Monaco, Principality of Monaco.

— (1995) The depositional environment of the evaporite mineral series at Tuzla, Bosnia-Herzegovina. Rapports de la Commission Internationale pour l'Exploration Scientifique de la Mer Méditerranée, 34, 105. Monaco, Principality of Monaco.

Smith, G.I. and Medrano, M.D. (1996) Continental borate deposits of Cenozoic age. In L.M.Anovitz and E.S.Grew, Eds., Boron: mineralogy, petrology and geochemistry, 33, 263–298. Reviews in Mineralogy, Mineralogical Society of America, Washington, D.C.

Warren, J. (1999) Evaporites—their evolution and economics. Blackwell Science, Oxford. 448 pages.

MANUSCRIPT RECEIVED JUNE 18, 2001

MANUSCRIPT ACCEPTED NOVEMBER 11, 2002

MANUSCRIPT HANDLED BY CELIA MERZBACHER